HHS Public Access

Author manuscript

Inhal Toxicol. Author manuscript; available in PMC 2017 December 28.

Published in final edited form as:

Inhal Toxicol. 2017 March ; 29(4): 169–178. doi:10.1080/08958378.2017.1333548.

Application of the ICRP respiratory tract model to estimate pulmonary retention of industrially sampled indium-containing dusts

Aleksandr B. Stefaniak, **M. Abbas Virji**, **Melissa A. Badding**, and **Kristin J. Cummings**

National Institute for Occupational Safety and Health, Centers for Disease Control and Prevention, Morgantown, WV, USA

Abstract

Inhalation of indium-containing dusts is associated with the development of indium lung disease. Workers may be exposed to several different chemical forms of indium; however, their lung dosimetry is not fully understood. We characterized the physicochemical properties and measured the lung dissolution kinetics of eight indium-containing dusts. Indium dissolution rates in artificial lung fluids spanned two orders of magnitude. We used the International Commission on Radiological Protection (ICRP) human respiratory model (HRTM) to estimate pulmonary indium deposition, retention and biokinetic clearance to blood. For a two-year (median workforce tenure at facility) exposure to respirable-sized particles of the indium materials, modeled indium clearance (>99.99% removed) from the alveolar-interstitial compartment was slow for all dusts; salts would clear in 4 years, sintered indium–tin oxide (ITO) would clear in 9 years, and indium oxide would require 48 years. For this scenario, the ICRP HRTM predicted that indium translocated to blood would be present in that compartment for 3.5–18 years after cessation of exposure, depending on the chemical form. For a 40-year exposure (working lifetime), clearance from the alveolar–interstitial compartment would require 5, 10 and 60 years for indium salts, sintered ITO and indium oxide, respectively and indium would be present in blood for 5–53 years after exposure. Consideration of differences in chemical forms of indium, dissolution rates, alveolar clearance and residence time in blood should be included in exposure assessment and epidemiological studies that rely on measures of total indium in air or blood to derive risk estimates.

Keywords

Inhalation; dissolution; indium; ITO; biodurability; dose metrics

CONTACT: Aleksandr B. Stefaniak, AStefaniak@cdc.gov, National Institute for Occupational Safety and Health, Centers for Disease Control and Prevention, Mailstop H-2800, Morgantown, WV 26505, USA.

Disclosure statement

The authors declare that they have no competing interests, financial or otherwise.

Supplemental data for this article can be accessed here.

Introduction

Indium–tin oxide (ITO) has exceptional optical and electrical properties, which make it ideal for use as a transparent thin film conductor in consumer electronics. In commercial practice, indium oxide and tin oxide powders are blended, compacted and sintered to make ITO. Off-specification or worn product and other indium-containing scrap materials are recycled to reclaim indium (Cummings et al., 2010; Miyauchi et al., 2012). During the production and reclamation of ITO, workers may inhale airborne dusts that contain indium metal, indium salts, indium hydroxide ($In(OH)_3$), indium oxide (In_2O_3) and/or ITO (Choi et al., 2015; Chonan et al., 2007; Cummings et al., 2010; Hamaguchi et al., 2008; Homma et al., 2003, 2005; Liu et al., 2012; Miyauchi et al., 2012; Nakano et al., 2009). Once inhaled, indium clears from the body slowly over time and hence persists in the body even after exposure ceases (Amata et al., 2015; Liu et al., 2016; Nakano et al., 2014). Some persons who inhale indium-containing dusts may develop indium lung disease, a severe and sometimes fatal condition characterized by pulmonary alveolar proteinosis (PAP), fibrosis and/or emphysema (Choi et al., 2013; Cummings et al., 2010; Homma et al., 2003; Liu et al., 2012; Nakano et al., 2016; Omae et al., 2011).

Epidemiologic studies have found adverse respiratory health outcomes associated with nonspecific exposure metrics, such as the concentration of indium in blood matrices or workplace air independent of chemical form (Chonan et al., 2007; Cummings et al., 2014, 2016; Nakano et al., 2009). Limited evidence from the literature suggests that toxicity of indium compounds may be influenced by the particle size (as it relates to regional lung deposition) as well as the form of indium, its physicochemical properties and dissolution (biodurability) in lung fluids (Andersen et al., 2017; Badding et al., 2014; Gwinn et al., 2013; Lim et al., 2014; Lison et al., 2009; Nagano et al., 2011; Tanaka et al., 2002, 2010). Unfortunately, little is understood or known about the physicochemical properties and dissolution behavior of real-world indium-containing dusts to which workers are exposed (Omae et al., 2011). Such data are necessary to better understand inhaled dose and disease risk from exposure to indium. In this study, we characterized the physicochemical properties and measured the dissolution of indium from particles encountered during the production and reclamation of ITO in artificial lung fluids and used this data to model deposition and time-dependent pulmonary indium, clearance and retention to illustrate the effects of dissolution characteristics of the chemical forms of indium on dose estimates.

Materials and methods

Eight study materials were collected from a facility that produces ITO and where two workers developed PAP (Cummings et al., 2010). At this facility, $In(OH)_3$ powder is used to make In_2O_3 powder which is mixed with tin oxide (SnO_2) powder and homogenized. The homogenized material is then formed into a desired shape. These unsintered shapes are sanded and then fired to produce sintered ITO. The sintered ITO shapes are machined to final dimensional specifications. Product that does not meet specifications, indium-containing wastes and worn product purchased back from customers are reclaimed by a proprietary process.

Study powder characterization

Eight indium-containing materials were collected at the facility as reported in a previous study (Badding et al., 2014). Three bulk materials were collected from the refinery (feedstock $In(OH)_3$, In_2O_3 and SnO_2 powders) at this facility. Two bulk material samples were collected from production processes: unsintered ITO (UITO) dust from a sanding operation and sintered ITO (SITO) dust from a machining operation. Three additional bulk materials were collected from the reclamation process: a mixture of waste sintered and unsintered (SUITO) dust, aerosol particles captured in a ventilation dust (VD) collector and reclaim by-product (RB) dust (Badding et al., 2014).

Particle size, density, surface area and surface chemistry of these materials were summarized previously (Badding et al., 2014). For the current study, materials were additionally characterized using scanning electron microscopy (SEM) with semiquantitative energy-dispersive X-ray analysis (EDX) to identify elemental constituents and with powder X-ray diffraction to identify crystalline constituents and specific phases (EB Scientific Enterprises, Golden, CO). Phase identifications were made by comparing the measured diffraction spectra to patterns in the International Centre for Diffraction Data Powder Diffraction File (ICDD, Newtown Square, MA) and to pertinent literature. The mass fraction of powder that was elemental indium and/or tin was determined using proton-induced X-ray emission (PIXE) spectroscopy (Elemental Analysis Corp., Lexington, KY).

Biodurability in artificial lung fluids

To evaluate the dissolution of indium and tin from particles that are inhaled and deposited in the conducting airways, we used a model of airway epithelial-lining fluid referred to as serum ultrafiltrate (SUF) (Finch et al., 1988). This formulation includes sodium citrate and the chelator DTPA, originally added to ensure that dissolved trivalent cations remained in solution. Results of animal studies (Gwinn et al., 2013; Nagano et al., 2011; Tanaka et al., 2002), cellular *in vitro* studies (Gwinn et al., 2013) and human lung biopsy specimens (Homma et al., 2003) indicate that indium-containing particles with size capable of penetrating to the alveolar region of the lung are engulfed and sequestered by macrophages. As such, dissolution of indium from particles was also evaluated using phagolysosomal simulant fluid (PSF) to mimic the acidic environment inside of alveolar macrophage phagolysosomes (Stefaniak et al., 2005). In a preliminary study with PSF, it was observed that up to 70% of a dissolved indium standard adhered to the containers used to perform the dissolution experiment and for sample storage prior to quantification; however, when sodium citrate and DTPA were added to PSF (at the same concentrations as prescribed for SUF), recovery of the indium standard was 90%. Hence, the PSF formulation originally described by Stefaniak et al. (2005) was modified to include sodium citrate (0.0588 g/L) and DTPA (0.0787 g/L) for all dissolution studies.

Each study material was evaluated using the well-established static dissolution technique as described previously (Kanapilly et al., 1973). A known mass of powder was weighed in a static dissolution chamber and each chamber immersed in 80 mL of artificial lung fluid maintained at 37 °C to mimic lung temperature. The SUF solvent was maintained at pH 7.4 ± 0.2 using 5% CO_2/95% air and samples of the liquid were collected at 3, 6, 12, 24, 48, 96

and 168 h. The PSF solvent remained at pH 4.5 ± 0.1 and samples were collected at 3, 6, 12, 18, 24, 48 and 96 h then weekly for 28 days to simulate long-term phagolysosomal sequestration during the lifespan of alveolar macrophages. Triplicate samples of each study material and field blanks (dissolution chambers without powder) were prepared for each dissolution experiment.

The initial mass of elemental indium and/or tin in each sample was calculated as the product of powder mass weighed into each dissolution chamber multiplied by the fraction of metal determined by PIXE analysis. Artificial lung fluid samples were analyzed without digestion to quantify the mass of dissolved metal using inductively coupled plasma-optical emission spectroscopy (ICP-OES). The matrix-specific limit of detection (LOD) and limit of quantification (LOQ) for indium were 10 and 48 μg/L (SUF) and 6 and 20 μg/L (PSF). For tin in SUF, the LOD and LOQ values were 10 and 47 μg/L (SUF). Note that based on the results from the study with SUF, it was observed that the dissolution of indium from particles was independent of the dissolution of tin (data not shown). Recently, Andersen et al. reported that the dissolution of indium and tin were independent from ITO particles (Andersen et al., 2017). Given that there was no interference with indium dissolution, tin was not quantified in the study with PSF. Neither indium nor tin was detected in any of the field or reagent blank samples.

For each material, values of the mass fraction of material remaining were plotted versus time and multiple-component negative exponential functions fitted to the data using the Proc NLIN procedure in SAS version 9.3 (SAS Institute, Cary, NC) and Sigma Plot version 12.5 (Systat Software Inc., San Jose, CA) (Chazel et al., 2000):

$$\text{fraction remaining} = f_r \cdot \exp(s_r t) + f_s \cdot \exp(s_s t) \quad (1)$$

where f = the proportion of the total element dissolved in the initial rapid (f_r) or latter slower ($f_s = 1 - f_r$) dissolution phase, s = the dissolution rate for the initial rapid (s_r) or latter slower (s_s) phase in d^{-1} and t = elapsed time (d). Values of f_r and f_s were determined from the intercepts of the fitted curves. The material fractional dissolution rates (s_r and s_i) were equal to the slopes of the fitted curves. Particle dissolution half-times ($t_{1/2}$) were calculated from the relationship $\frac{\ln 2}{\text{slope}}$.

Lung dosimetry modeling

A major objective of this study was to highlight the effect of material form on dose. Though particle size distribution, density and other physical factors are important for estimating pulmonary deposition, the focus herein was not to estimate dose in a specific region of the lung to evaluate some toxicological end point, rather it was to illustrate the effect of chemical form and its importance for exposure assessment and generation of metrics for epidemiologic studies. To achieve this objective, particle deposition and clearance in the respiratory tract were modeled using the Activity and Internal Dose Estimates (AIDE) software (Bertelli et al., 2008). The software uses the International Commission on Radiological Protection (ICRP) human respiratory tract model (HRTM) to calculate the mass of indium remaining in the different respiratory tract compartments (lung burden) and

accounts for mechanical clearance and dissolution clearance in biological fluids (ICRP, 1994). The ICRP model uses a simplistic lung morphometry assuming the lung acts as a series of filters that dictate regional lung deposition for particles across a range of sizes (Supplemental Figure S1a). Since clearance from the tracheobronchial and head airways compartments are relatively rapid and indium lung disease is manifest primarily in the alveoli, we focused on long-term dose from exposure to respirable size particles, that is, mass median aerodynamic diameter (MMAD) = 4 and geometric standard deviation (GSD) = 2.5. Rather than use the ICRP default MMAD of 5 μm, we defined respirable size particles as having a MMAD of 4 μm based on the convention for "respirable" air samplers, which have a 50% collection efficiency at that diameter (Lippman, 1999). In this situation, the GSD of 2.5 has more influence than the MMAD in modeled particle lung deposition. For example, at a GSD of 2.5 the alveolar regional deposition (compartment of interest for indium lung disease) values are 9.9% and 9.6% for 4 and 5 μm particles, respectively. Note that in addition to the size distribution, density can exert significant influence on particle regional lung deposition, especially for scenarios in which particle sizes are small and in the Stokes regime (Miller et al., 2013). A range of densities were previously measured for the indium study materials (Badding et al., 2014). For the case when the exposure material is In_2O_3 particles with a density of 7.18 g/cm^3, then a particle with aerodynamic diameter of 4 μm will have a physical particle size of 1.44 μm. At the lower end of measured densities, if the exposure material is particles of $In(OH)_3$ with a density of 4.38 g/cm^3, then the physical diameter for these lower density particles is 1.87 μm. Hence, in this situation, for the indium facility under study, even though the different densities of these materials results in different physical diameters for particles of the same aerodynamic diameter, those particles will behave the same in terms of their regional deposition in the human respiratory tract. For mechanical clearance, the default rate constants were obtained from the ICRP HRTM (see Supplemental Figure S1b). For the biokinetic components of the model, additional code was obtained from the author of the software to implement the systemic distribution and clearance of indium by ICRP 30. The fractional coefficients were: marrow 0.3, liver 0.2, kidney 0.07, spleen 0.02 and other organs 0.41 with indefinite retention in the organs (ICRP, 1981). Hoet et al. and Castronovo and Wegner reported that indium kinetics in the blood followed a biphasic clearance with half-lives of 1.9 to 2.8 days for the fast phase and 60 to 69 days for the slow phase (Castronovo & Wagner, 1973; Hoet et al., 2012). Thus, rather than using a fractional clearance rate for indium in blood of 2.77 d^{-1} (half-life of 0.25 days) we used 0.011 d^{-1} (half-life of 65 days) as the slower rate is more consistent with the protracted release of poorly soluble forms of indium from the lungs as well as evidence from human data showing prolonged presence of indium in blood years after the cessation of exposure (further, the software cannot accommodate biphasic clearance) (Hoet et al., 2012). The use of a single clearance rate constant of 0.011 d^{-1} provides a reasonable estimate for modeling clearance from the respiratory tract of both acutely and chronically exposed workers. For chemical clearance (see Supplemental Figure S1c), the material-specific indium dissolution rates (d^{-1}) and fractions were obtained from the dissolution studies. The AIDE software only permits input of a single set of dissolution parameters for all respiratory compartments. For modeling purposes, we used the rates and fractions determined from the PSF studies because, as noted above, indium lung disease is primarily manifest in the alveoli.

Modeling was performed assuming a reference worker at light work, breathing through their nose only and following a pattern of 8 h of exposure (deposition and clearance) followed by 16 h of clearance each day for 5 work days followed by 2 days off representing clearance only. Two exposure scenarios were modeled. In the first, exposure duration was taken to be 2 years, the median tenure for the workforce at this facility (Cummings et al., 2014), followed by a clearance period of 53 years. In the second scenario, exposure duration was 40 years (working lifetime) followed by a clearance period of 15 years for the faster clearing VD dust to 60 years for the slower clearing indium oxide. For the purposes of this study, clearance was considered to be complete when the amount of indium remaining in a respiratory tract compartment or blood reached 0.01% of the initial mass inhaled. Though we focused on a light work scenario as this is the predominate type of work at this facility, breathing rate influences deposition and the same scenarios described herein were modeled for a heavy breathing (100% nose breather) worker and results are provided in Supplemental File 2. The mass fraction of indium distributed among various respiratory tract compartments and to blood were plotted against time using Sigma Plot to explore dose and retention patterns for the different exposure scenarios.

Results

Differences in physicochemical properties among forms of indium encountered in the workplace translated into differences in observed indium dissolution from the study samples, which in turn, influenced lung dose and clearance kinetics.

Study powder characteristics

All bulk materials were composed of particles with sizes capable of penetrating to the alveolar region of the lung (Badding et al., 2014). On the surfaces of the three ITO materials, indium was present as a mixture of indium metal (In^0) and In_2O_3 at similar proportions; tin was present in the form of SnO (not SnO_2). The VD collector and RB particle surfaces were consistent with indium salt and In_2O_3 (also In^0 on the surface of the RB dust). Elemental analysis by EDX confirmed that the feedstock powders were high purity (i.e. indium to oxygen ratios approached values expected from stoichiometry). Assuming that the ITO powders were a 90:10 mixture of In_2O_3 and SnO_2, the ratios of indium to oxygen and tin to oxygen also indicated high-purity materials. The VD particles gave strong EDX signals indicating that this material contained an indium salt and the RB dust produced weaker signals indicative of lower amounts of the indium salt. From X-ray diffraction analysis, the feedstock indium hydroxide, indium oxide and tin oxide were pure crystalline $In(OH)_3$, In_2O_3 and SnO_2, respectively. All ITO materials were crystalline cubic In_2O_3 and SnO_2. The particles from the VD collector contained crystalline In_2O_3. The diffraction pattern of RB dust was consistent with a highly crystalline material though none of the peaks matched reference patterns for In_2O_3, SnO_2 or ITO. PIXE analysis revealed that the indium or tin content of the feedstock powders matched values based on stoichiometry. Levels of indium in the ITOs were similar. Among the eight study materials, levels of tin ranged from 0.3% (VD) to 8% (SUITO, SITO).

Dissolution in simulated lung fluids

As shown in Figure 1(a–c), dissolution of indium from all indium-containing study powders in SUF was biphasic, that is, consisted of an initial rapid phase followed by a later slower phase. Tin dissolution followed the same bi-phasic pattern (data not shown). In SUF, the total mass of indium dissolved was greatest from the VD and RB materials (Figure 1(a)), intermediate for $In(OH_3)$, UITO and SITO (Figure 1(b)) and least for In_2O_3 and SUITO (Figure 1(c)). Interestingly, the mass fractions of dissolved indium differed among the ITOs despite having the same crystalline phase of indium and nearly identical surface and bulk chemistries. As shown in Table 1, the rank order of specific surface areas of the ITOs were (from highest to lowest) UITO >SITO >SUITO. Hence, the greater the available surface area for solvation, the more indium that dissolved, which explains the observed differences in fractional dissolution rates among the ITO materials. Table 1 summarizes the cumulative amount of indium and/or tin dissolved, and the fitted dissolution parameters (f_r, f_s, s_r and s_s) for the industrially sampled powders in SUF. The calculated values of s_r for indium varied from 0.25 to 6.15 d^{-1} among study materials. Values of s_s for indium spanned two orders of magnitude.

Based on the SUF data, three representative indium-containing materials that spanned the range of observed solubilities (VD, SITO and In_2O_3) were further evaluated in PSF to understand the alveolar fate of indium. As shown in Figure 1(d), in PSF dissolution of indium from In_2O_3, SITO and VD particles was biphasic. As summarized in Table 2, the mass fractions of indium that dissolved differed by material and followed the rank order (from greatest to least): VD >SITO >In_2O_3. For each material tested in the acidic PSF model, the mass fraction of indium dissolved was greater than in SUF at near-neutral pH. Table 2 also summarizes the fitted dissolution parameters for these materials that were used to model lung dosimetry.

Lung dose metrics

Figure 2(a) is a plot of alveolar indium retention predicted by the ICRP HRTM for a two-year (median tenure) exposure to respirable sized particles of In_2O_3, SITO and VD particles. The clearance aspect of the model includes the contributions from both indium chemical dissolution (as measured in PSF) and mechanical particle removal mechanisms (i.e. particle biopersistence). From this plot, indium lung clearance rates in the alveolar compartment were slow for all study powders though long-term indium retention differed among chemical forms. Specifically, three distinct alveolar retention profiles for indium were evident. Following cessation of exposure, indium in the form of salts in VD particles would need 4 years to clear, indium in the form of SITO would clear in 9 years and indium as In_2O_3 would require 48 years.

Of interest is the slow clearance of indium from blood following a two-year exposure as shown in Figure 2(b) because this matrix is often used as a biological marker of exposure (Harvey et al., 2016). In the ICRP HRTM, indium clearance to blood is a reflection of only the chemical dissolution rate. Note that our modeling results are based only on measurements in PSF because our emphasis was on alveolar aspects of indium lung disease and *in vivo* dissolution in the airway lining fluid (mimicked by SUF) is only relevant for the

first few days following particle deposition, as such, dissolution by alveolar macrophages (mimicked by PSF) would mainly contribute to indium clearance to blood. The ICRP model predicted that following two years of exposure to indium in the form of VD, SITO and In_2O_3 indium would remain in blood for 3.5, 6.5 and 18 years, respectively and is systemically distributed to other organs in the body over time.

For a 40-year exposure (Figure 2(c)), the ICRP HRTM predicted that indium would quickly accumulate in the alveoli before reaching a plateau. The same three general alveolar retention profiles by chemical form of indium compound were also observed for a 40-year exposure. After cessation of 40 years of exposure, the model predicted it would take 5 years to clear the indium from the alveoli for VD particles, 10 years for SITO particles and 60 years for In_2O_3.

Figure 2(d) presents plots of blood indium retention predicted by the ICRP model for a 40-year (working lifetime) exposure to respirable size particles. For this scenario, the model predicted that following exposure to indium in the form of VD, SITO and In_2O_3 indium would remain in blood for 5, 10 and 53 years, respectively.

The model results presented in Figure 2 are for a reference worker at light work; however, some jobs at this facility require more exertion, which will affect breathing patterns and therefore particle deposition and indium retention. To understand the influence of work pattern on indium retention, we modeled alveolar and plasma indium on fractional retention for VD, SITO and In_2O_3 indium dusts under heavy exercise and 100% nose breather (see Figure S1 in the Supplemental File) for the same 2- and 40-year exposure scenarios as described earlier. Among the forms of indium dusts, for the 2-year exposure scenario, heavy exercise increased indium retention in the alveoli by 31–36% compared to light work and increased plasma retention by 22–35%. For the 40-year exposure scenario, heavy exercise increased indium retention in the alveoli by 34–37% and indium retention in the plasma by 24–35%.

Discussion

Workers engaged in the production and reclamation of ITO are potentially exposed to indium having a variety of chemical forms (Choi et al., 2015; Chonan et al., 2007; Cummings et al., 2010; Hamaguchi et al., 2008; Homma et al., 2003, 2005; Liu et al., 2012; Miyauchi et al., 2012; Nakano et al., 2009). Our *in vitro* experiments demonstrated that indium was released from all tested study materials using SUF or PSF artificial lung fluids and that observed differences in dissolution rates could be attributed to the chemical form of indium in the dust. For example, the VD and RB dusts which contained indium in the form of a salt were most soluble, whereas the feedstock In_2O_3 which contained highly crystalline In_2O_3 was the least soluble.

Previously, it was reported that commercially available unsintered ITO particles were rapidly engulfed by the RAW 264.7 macrophage cell line *in vitro* (Gwinn et al., 2013). Rapid uptake by macrophages of the same indium-containing particles used in the present study was confirmed *in vitro* (Badding et al., 2015). In the study of commercially available unsintered

ITO particles, Gwinn et al. measured ionic indium in culture media following particle uptake and reported that dissolution in macrophage phagolysosomes was a key driver for cytotoxicity (Gwinn et al., 2013). In a follow-on study by the same group, macrophage-mediated dissolution of sintered ITO particles and indium phosphide particles was reported to predict pulmonary toxicity *in vivo* (Gwinn et al., 2015). In a study of In_2O_3 nanoparticles, it was reported that the slow *in vitro* indium dissolution rate observed in artificial phagolysosomal fluid (pH 5.5) was consistent with the *in vivo* persistence of these particles in rats and the time course of development of PAP (Jeong et al., 2016). In our study, we also observed faster indium dissolution under acidic conditions (pH 4.5) compared to near-neutral conditions (pH 7.4) and Andersen et al. recently reported the same observation for a commercially available ITO powder (Andersen et al., 2017). Collectively, these data indicate that in the tracheobronchial (conducting airways) region, clearance by mechanical processes will dominate whereas in the nonciliated alveolar region of the lung, chemical dissolution inside macrophage phagolysosomes will contribute more to clearance. Regardless of lung fluid model, the indium-containing dusts exhibited three distinct categories of low, intermediate, and somewhat higher solubility (Figure 1) which indicates that indium retention in the lung differs among chemical forms and their physicochemical properties. A recent study by Badding et al. revealed differences in plasma indium concentrations over a time course of 90 days in rats exposed to a bolus intratracheal instillation dose of the In_2O_3, SITO and VD particles used in the current study (Badding et al., 2016). Substantially larger concentrations of indium were detected in early blood measurements (days 1 and 7) with VD exposure versus In_2O_3 or SITO, which may reflect the enhanced dissolution of indium from those particles. Furthermore, the same dose level of In_2O_3 resulted in negligible amounts of blood indium, suggesting slow indium dissolution in the lungs of rats.

Available case reports and epidemiological studies indicate that persons who inhale indium-containing dusts may develop indium lung disease (Choi et al., 2013; Cummings et al., 2010; Homma et al., 2003; Liu et al., 2012; Nakano et al., 2016; Omae et al., 2011); however, disease has not been causally linked to a specific chemical form of indium. Specifically, it is unclear if all forms of indium are capable of inducing PAP and fibrosis, and therefore, pose the same disease risk. Prior to this report, little was known about the physicochemical properties and dissolution behavior of real-world indium-containing dusts to which workers were exposed. Our data document five different chemical forms of indium (salts, metal, hydroxide, oxide or alloyed with tin) present in various dusts encountered during production and reclamation of ITO at one facility. Use of the ICRP HRTM enabled us to predict pulmonary retention based on material-specific dissolution parameters and mechanical clearance mechanisms. All chemical forms of indium required years to clear from the lung after cessation of exposure (Figure 2). Notably, clearance rates were slowest from the alveolar lung compartment, which is the site of clinical manifestation for indium lung disease (Cummings et al., 2012). If a long-term indium burden in the lung contributes to indium lung disease, particularly advanced findings of fibrosis and emphysema (Cummings et al., 2012; Nakano et al., 2014), then our data suggest that all forms of indium identified in these dusts may contribute to burden and pose a health risk. Indeed, fibrotic lesions were evident in the lungs of rats exposed to indium-containing particles with a range of dissolution rates (In_2O_3, SITO, or VD) (Badding et al., 2016). However, the

histopathological analysis suggested differential severity, with rats exposed to SITO and VD scoring higher for PAP and fibrosis compared to In_2O_3 at the same dose. Alternatively, if intra-alveolar accumulation of surfactant and impairment of lung function characteristic of indium lung disease is triggered by a specific underlying mechanism, then perhaps only specific forms of indium could induce such reactions. Findings from our *in vitro* (Badding et al., 2015) and *in vivo* (Badding et al., 2016) studies have demonstrated compromised phagocytic function of macrophages following exposure to SITO and VD particles but not with other indium-containing particles. Given that impaired phagocytosis contributes to disturbed surfactant homeostasis and has been implicated in PAP (Greenhill & Kotton, 2009; Kitamura et al., 1999), macrophage dysfunction may be a key initiator in the pathogenesis of indium lung disease. It is worth mentioning that available literature documents the presence of indium-containing particulate in lung tissue of exposed workers and biopsy specimens of experimental animals for months to years after last exposure (Badding et al., 2016; Hoet et al., 2012; Homma et al., 2003; Tanaka et al., 2010). Our dissolution data (Tables 2 and 3) confirm that indium-containing particles encountered during production and reclamation of ITO are biodurable in the lung and can persist in the alveoli for years after cessation of exposure. Note that the actual persistence of indium in the lung (and blood) may be different than predicted by HRTM because the model does not account for impaired mechanical clearance due to macrophage dysfunction or cytotoxicity from dissolution of indium.

Finally, the regional lung compartment and blood clearance rates predicted from the *in vitro* dissolution data has implications for biomonitoring. Measurements of indium in whole blood, plasma or serum are often used as indices of inhalational exposure (Choi et al., 2013; Chonan et al., 2007; Cummings et al., 2014; Hamaguchi et al., 2008; Harvey et al., 2016; Hoet et al., 2012; Homma et al., 2003, 2005; Iwasawa et al., 2017; Liao et al., 2004; Liu et al., 2012; Miyaki et al., 2003; Nakano et al., 2009). The underlying premise of these biomarkers is that indium-containing particles that deposit in the lung undergo dissolution and the solubilized indium ions are transferred to blood and excreted so they can be used as a measure of exposure (properly accounting for exposure and work history). Our dissolution and clearance data indicate several important points that must be considered when interpreting indium biomonitoring results from blood matrices: (1) all forms of indium encountered in a workplace will contribute to blood indium burden, though at different rates; (2) the concentration of indium in blood is influenced by the chemical form of indium to which a worker is exposed and by the burden of indium in the lungs; and (3) indium clearance from blood occurs over a period of years and is therefore not an indicator of current exposure. The importance of this latter point is highlighted by a report that the clearance half-time for indium in serum was 8.1 years in former workers (Amata et al., 2015). As such, these data present an initial effort to provide a dissolution-based explanation as to why blood indium levels may not directly relate to current airborne exposure (Hoet et al., 2012) and thus may not be representative of lung dose over shorter time periods, particularly in workers with longer employment tenure.

Our software model can only use one set of dissolution parameters and by choosing the faster PSF values to predict clearance it can result in an over estimation of dissolution clearance and slightly over estimate blood levels. On the other hand, clearance from blood only is based on the slower rate of the biphasic clearance which accounts for 69% of the

clearance, thus leading to under estimation of the dissolution clearance (Castronovo & Wagner, 1973). Moreover, the ICRP model assumes indefinite retention in the organs; however, an animal experiment by Hoet et al. 2012 (and citations therein of previous short-term exposure studies by Castronovo and Wagner) using a single exposure to In_2O_3 (pharyngeal aspiration) or $InCl_3$ (intraperitoneal injection) suggested there was evidence of a systemic depot in the organs which may contribute to blood indium levels which is not accounted for in this model (Hoet et al., 2012). Additionally, the fractional distribution of indium in the different organs are not consistent between the ICRP model and experimental studies by Hoet et al. and Castonovo and Wagner (Castronovo & Wagner, 1973; Hoet et al., 2012). The foregoing evidence suggests that, at this time, there are limitations with modeling blood indium values, though the overall patterns over time are informative and useful in interpreting biomonitoring data. For more realistic modeling of expected blood content under different exposure and work history scenarios, a more accurate physiologically based pharmacokinetic model is needed that accounts for contributions from systemic organs and indium recycling biokinetics.

In epidemiologic studies of chronic diseases, especially of cancer outcomes, cumulative exposure is an effective summary metric used in exposure-response models (Kriebel et al., 2007), but its use in noncancer outcomes is called to question (de Vocht et al., 2015). Cumulative exposure is based on several assumptions about the exposure disease association including a linear accumulation of dose at the target tissue (Smith, 1992). In this study, dose modeling for 40 years suggest that in the alveoli, an equilibrium (between accumulation and clearance) is reached with these poorly soluble materials in less than 10 years; dose does not increase infinitely with time. Cumulative exposure over periods longer than 10 years will likely overestimate exposure, which in turn will underestimate the measure of risk and flatten the exposure-response curve at the higher concentrations of cumulative exposure. Thus, dissolution characteristics can inform the creation of exposure metrics for use in epidemiologic studies. Moreover, the dose profile over time permits different exposure metrics to be created to explore different disease mechanisms and exposure response relationships.

Conclusions

Consistent with our hypothesis, differences in physicochemical properties of the indium-containing study materials evaluated herein translated into differences in dissolution and biokinetic behavior. Using the ICRP HRTM, three distinct alveolar clearance profiles were evident: indium in the form of salts from reclamation operations would clear fastest, followed by indium in the form of less soluble $In(OH)_3$, SITO and UITO and finally indium in the form of least soluble In_2O_3 and SUITO. The clearance of indium to blood was predicted to result in persistence in that compartment for years since last exposure and its retention depended on the chemical form of indium exposure material. We conclude that not all chemical forms of indium will dissolve and clear in the same manner, which is an important consideration for exposure assessment and epidemiological studies of indium workers that rely on measures of total indium in air or blood to derive risk estimates.

Supplementary Material

Refer to Web version on PubMed Central for supplementary material.

Acknowledgments

The authors wish to thank NIOSH staff members M.G. Duling and R.B. Lawrence for assistance with the dissolution studies and Dr. Ji Young Park for collection of the MOUDI samples. Mention of a specific product or company does not constitute endorsement by the Centers for Disease Control and Prevention. The findings and conclusions in this report are those of the authors and do not necessarily represent the views of NIOSH.

Funding

This project was funded by NIOSH through an intramural National Occupational Research Agenda grant. The decision to submit the manuscript for publication was that of the authors and was independent of the funding source or the company from which the study materials were obtained.

References

Amata A, Chonan T, Omae K, et al. High levels of indium exposure relate to progressive emphysematous changes: a 9-year longitudinal surveillance of indium workers. Thorax. 2015; 70:1040–6. [PubMed: 26286723]

Andersen JC, Cropp A, Paradise DC. Solubility of indium-tin oxide in simulated lung and gastric fluids: pathways for human intake. Sci Total Environ. 2017; 579:628–36. [PubMed: 27863865]

Badding MA, Fix NR, Orandle MS, et al. Pulmonary toxicity of indium-tin oxide production facility particles in rats. J Appl Toxicol. 2016; 36:618–26. [PubMed: 26472246]

Badding MA, Schwegler-Berry D, Park JH, et al. Sintered indium-tin oxide particles induce pro-inflammatory responses *in vitro*, in part through inflammasome activation. PLoS One. 2015; 10:e0124368. [PubMed: 25874458]

Badding MA, Stefaniak AB, Fix NR, et al. Cytotoxicity and characterization of particles collected from an indium-tin oxide production facility. J Toxicol Environ Health Part A. 2014; 77:1193–209. [PubMed: 25208660]

Bertelli L, Melo DR, Lipsztein J, Cruz-Suarez R. AIDE: internal dosimetry software. Radiat Prot Dosimetry. 2008; 130:358–67. [PubMed: 18337289]

Castronovo FP Jr, Wagner HN Jr. Comparative toxicity and pharmacodynamics of ionic indium chloride and hydrated indium oxide. J Nucl Med. 1973; 14:677–82. [PubMed: 4724336]

Chazel V, Houpert P, Ansoborlo E, et al. Variation of solubility, biokinetics and dose coefficient of industrial uranium oxides according to specific surface area. Radiat Prot Dosimetry. 2000; 88:223–31.

Choi S, Won YL, Kim D, et al. Interstitial lung disorders in the indium workers of Korea: an update study for the relationship with biological exposure indices. Am J Ind Med. 2015; 58:61–8. [PubMed: 25345911]

Choi S, Won YL, Kim D, et al. Subclinical interstitial lung damage in workers exposed to indium compounds. Ann Occup Environ Med. 2013; 25:24. [PubMed: 24472147]

Choi S, Won YL, Kim EA. Effect of respiratory protector intervention among indium reclaiming workers. Am J Ind Med. 2015; 58:1319–20. [PubMed: 26442982]

Chonan T, Taguchi O, Omae K. Interstitial pulmonary disorders in indium-processing workers. Eur Respir J. 2007; 29:317–24. [PubMed: 17050566]

Cummings KJ, Donat WE, Ettensohn DB, et al. Pulmonary alveolar proteinosis in workers at an indium processing facility. Am J Respir Crit Care Med. 2010; 181:458–64. [PubMed: 20019344]

Cummings KJ, Nakano M, Omae K, et al. Indium lung disease. Chest. 2012; 141:1512–21. [PubMed: 22207675]

Cummings KJ, Virji MA, Park JY, et al. Respirable indium exposures, plasma indium, and respiratory health among indium-tin oxide (ITO) workers. Am J Ind Med. 2016; 59:522–31. [PubMed: 27219296]

Cummings KJ, Virji MA, Trapnell BC, et al. Early changes in clinical, functional, and laboratory biomarkers in workers at risk of indium lung disease. Ann Am Thorac Soc. 2014; 11:1395–403. [PubMed: 25295756]

de Vocht F, Burstyn I, Sanguanchaiyakrit N. Rethinking cumulative exposure in epidemiology, again. J Expo Sci Environ Epidemiol. 2015; 25:467–73. [PubMed: 25138292]

Finch GL, Mewhinney JA, Eidson AF, et al. In vitro dissolution characteristics of beryllium oxide and beryllium metal aerosols. J Aerosol Sci. 1988; 19:333–42.

Greenhill SR, Kotton DN. Pulmonary alveolar proteinosis: a bench-to-bedside story of granulocyte-macrophage colony-stimulating factor dysfunction. Chest. 2009; 136:571–7. [PubMed: 19666756]

Gwinn WM, Qu W, Bousquet RW, et al. Macrophage solubilization and cytotoxicity of indium-containing particles as in vitro correlates to pulmonary toxicity in vivo. Toxicol Sci. 2015; 144:17–26. [PubMed: 25527823]

Gwinn WM, Qu W, Shines CJ, et al. Macrophage solubilization and cytotoxicity of indium-containing particles in vitro. Toxicol Sci. 2013; 135:414–24. [PubMed: 23872580]

Hamaguchi T, Omae K, Takebayashi T, et al. Exposure to hardly soluble indium compounds in ITO production and recycling plants is a new risk for interstitial lung damage. Occup Environ Med. 2008; 65:51–5. [PubMed: 17626138]

Harvey RR, Virji MA, Edwards NT, Cummings KJ. Comparing plasma, serum and whole blood indium concentrations from workers at an indium-tin oxide (ITO) production facility. Occup Environ Med. 2016; 73:864–7. [PubMed: 27456157]

Hoet P, De Graef E, Swennen B, et al. Occupational exposure to indium: what does biomonitoring tell us? Toxicol Lett. 2012; 213:122–8. [PubMed: 21771645]

Homma S, Miyamoto A, Sakamoto S, et al. Pulmonary fibrosis in an individual occupationally exposed to inhaled indium-tin oxide. Eur Respir J. 2005; 25:200–4. [PubMed: 15640342]

Homma T, Ueno T, Sekizawa K, et al. Interstitial pneumonia developed in a worker dealing with particles containing indium-tin oxide. J Occup Health. 2003; 45:137–9. [PubMed: 14646287]

ICRP. International Commission on Radiological Protection. Publication 30 (Part 3): Limits for intakes of radionuclides by workers. Ann ICRP. 1981; 6(2–3)

ICRP. Publication 66: Human respiratory tract model for radiological protection. Oxford (UK): Pergamon; 1994. International Commission on Radiological Protection.

Iwasawa S, Nakano M, Miyauchi H, et al. Personal indium exposure concentration in respirable dusts and serum indium level. Ind Health. 2017; 55:87–90. [PubMed: 27644848]

Jeong J, Kim J, Seok SH, Cho WS. Indium oxide (In_2O_3) nanoparticles induce progressive lung injury distinct from lung injuries by copper oxide (CuO) and nickel oxide (NiO) nanoparticles. Arch Toxicol. 2016; 90:817–28. [PubMed: 25731971]

Kanapilly GM, Raabe OG, Goh CH, Chimenti RA. Measurement of in vitro dissolution of aerosol particles for comparison to in vivo dissolution in the lower respiratory tract after inhalation. Health Phys. 1973; 24:497–507. [PubMed: 4707664]

Kitamura T, Tanaka N, Watanabe J, et al. Idiopathic pulmonary alveolar proteinosis as an autoimmune disease with neutralizing antibody against granulocyte/macrophage colony-stimulating factor. J Exp Med. 1999; 190:875–80. [PubMed: 10499925]

Kriebel D, Checkoway H, Pearce N. Exposure and dose modelling in occupational epidemiology. Occup Environ Med. 2007; 64:492–8. [PubMed: 17582090]

Liao YH, Yu HS, Ho CK, et al. Biological monitoring of exposures to aluminium, gallium, indium, arsenic, and antimony in opto-electronic industry workers. J Occup Environ Med. 2004; 46:931–6. [PubMed: 15354058]

Lim CH, Han JH, Cho HW, Kang M. Studies on the toxicity and distribution of indium compounds according to particle size in Sprague-Dawley rats. Toxicol Res. 2014; 30:55–63. [PubMed: 24795801]

Lippman, M. Rationale for particle size-selective aerosol sampling. In: Vincent, J., editor. Particle size-selective sampling for particulate air contaminants. Cincinnati, OH: ACGIH; 1999. p. 3-28.

Lison D, Laloy J, Corazzari I, et al. Sintered indium-tin-oxide (ITO) particles: a new pneumotoxic entity. Toxicol Sci. 2009; 108:472–81. [PubMed: 19176593]

Liu HH, Chen CY, Chen GI, et al. Relationship between indium exposure and oxidative damage in workers in indium tin oxide production plants. Int Arch Occup Environ Health. 2012; 85:447–53. [PubMed: 21833746]

Liu HH, Chen CY, Lan CH, et al. Effects of a powered air-purifying respirator intervention on indium exposure reduction and indium related biomarkers among ITO sputter target manufacturing workers. J Occup Environ Hyg. 2016; 13:346–55. [PubMed: 26771526]

Miller FJ, Kaczmar SW, Danzeisen R, Moss OR. Estimating lung burdens based on individual particle density estimated from scanning electron microscopy and cascade impactor samples. Inhal Toxicol. 2013; 25:813–27. [PubMed: 24304308]

Miyaki K, Hosoda K, Hirata M, et al. Biological monitoring of indium by means of graphite furnace atomic absorption spectrophotometry in workers exposed to particles of indium compounds. J Occup Health. 2003; 45:228–30. [PubMed: 14646281]

Miyauchi H, Minozoe A, Tanaka S, et al. Assessment of work-place air concentrations of indium dust in an indium-recycling plant. J Occup Health. 2012; 54:103–11. [PubMed: 22322108]

Nagano K, Gotoh K, Kasai T, et al. Two- and 13-week inhalation toxicities of indium-tin oxide and indium oxide in rats. J Occup Health. 2011; 53:51–63. [PubMed: 21233592]

Nagano K, Nishizawa T, Eitaki Y, et al. Pulmonary toxicity in mice by 2- and 13-week inhalation exposures to indium-tin oxide and indium oxide aerosols. J Occup Health. 2011; 53:234–9. [PubMed: 21422720]

Nakano M, Omae K, Tanaka A, et al. Causal relationship between indium compound inhalation and effects on the lungs. J Occup Health. 2009; 51:513–21. [PubMed: 19834281]

Nakano M, Omae K, Uchida K, et al. Five-year cohort study: emphysematous progression of indium-exposed workers. Chest. 2014; 146:1166–75. [PubMed: 24946105]

Nakano M, Tanaka A, Hirata M, et al. An advanced case of indium lung disease with progressive emphysema. J Occup Health. 2016; 58:477–81. [PubMed: 27488043]

Omae K, Nakano M, Tanaka A, et al. Indium lung-case reports and epidemiology. Int Arch Occup Environ Health. 2011; 84:471–7. [PubMed: 20886351]

Smith TJ. Occupational exposure and dose over time: limitations of cumulative exposure. Am J Ind Med. 1992; 21:35–51. [PubMed: 1553984]

Stefaniak AB, Guilmette RA, Day GA, et al. Characterization of phagolysosomal simulant fluid for study of beryllium aerosol particle dissolution. Toxicol In Vitro. 2005; 19:123–34. [PubMed: 15582363]

Tanaka A, Hirata M, Homma T, Kiyohara Y. Chronic pulmonary toxicity study of indium-tin oxide and indium oxide following intratracheal instillations into the lungs of hamsters. J Occup Health. 2010; 52:14–22. [PubMed: 19940388]

Tanaka A, Hirata M, Omura M, et al. Pulmonary toxicity of indium-tin oxide and indium phosphide after intratracheal instillations into the lung of hamsters. J Occup Health. 2002; 44:99–102.

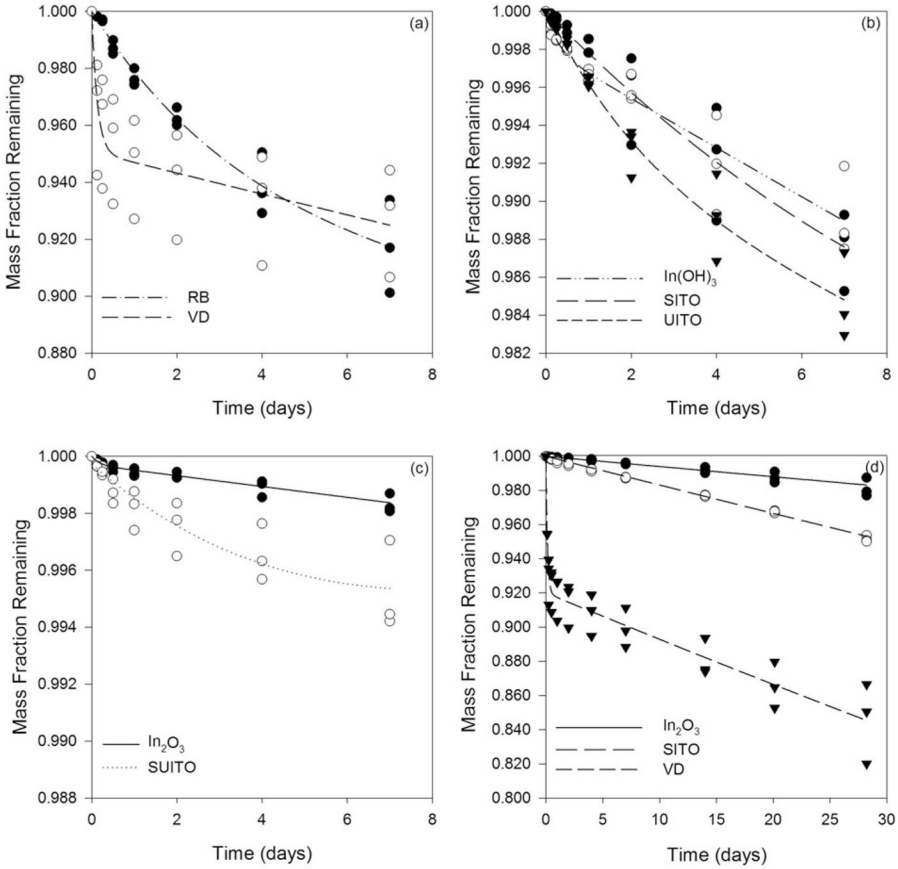

Figure 1.

Dissolution kinetics of indium in artificial lung fluids. Dissolution in SUF (pH 7.4) was biphasic and the mass fraction of indium that dissolved was: (a) greatest for VD and RB; (b) intermediate for $In(OH)_3$, SITO and UITO; and (c) least for In_2O_3 and SUITO. In PSF (pH 4.5), dissolution of In_2O_3 and SITO was linear and for VD it was biphasic; the mass fractions of indium dissolved were as follows: (d) VD >SITO >In_2O_3. Line in each plot for each material is the average fitted curve for $n = 3$ samples.

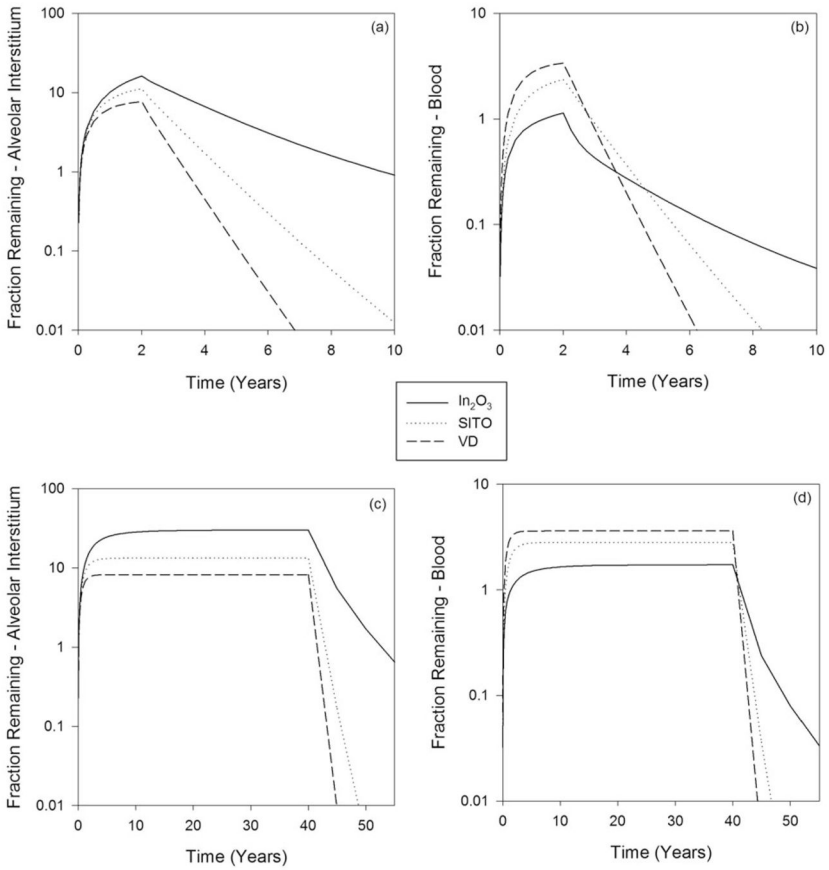

Figure 2.

Clearance predicted by the ICRP HRTM for respirable size particles of each study powder for a reference human at light work. Two-year exposure: (a) lung alveoli, (b) blood. Forty-year exposure: (c) lung alveoli, (d) blood.

Table 1

Dissolution of indium and tin from industrially-sampled powders (n = 3 samples per cell) in SUF (pH 7.4).

				Dissolution parameters (Mean ± Standard Deviation)[a]					
				Initial rapid phase			Latter slower phase		
Material[b]	**SSA (m^2/g)**[c]	**Element**	**Cum (%)**[d]	f_r (%)	$t_{1/2}$ (d)	s_r (d^{-1})	f_s (%)	$t_{1/2}$ (d)	s_s (d^{-1})
$In(OH)_3$	<25	Indium[e]	0.91 ± 0.19	0.3 ± 0.1	0.3 ± 0.2	2.97 ± 1.66	99.7 ± 0.1	831 ± 247	$8.8 \pm 2.6 \times 10^{-4}$
In_2O_3	<5	Indium	0.07 ± 0.01	0.02 ± 0.01	0.2 ± 0.1	4.83 ± 2.69	100.0 ± 0.0	10905 ± 4077	$6.7 \pm 2.3 \times 10^{-5}$
SnO_2	<10	Tin	0.36 ± 0.06	0.3 ± 0.1	0.4 ± 0.0	1.58 ± 0.03	99.7 ± 0.1	8165 ± 2355	$8.7 \pm 2.3 \times 10^{-5}$
UITO	<5	Indium	1.31 ± 0.14	1.1 ± 0.5	1.8 ± 0.6	0.44 ± 0.20	98.9 ± 0.6	1169 ± 540	$6.7 \pm 3.0 \times 10^{-4}$
		Tin	1.64 ± 0.51	1.4 ± 0.4	0.6 ± 0.1	1.12 ± 0.11	98.6 ± 0.4	2030 ± 807	$3.9 \pm 1.8 \times 10^{-4}$
SITO	3.0 ± 0.1	Indium	0.96 ± 0.34	1.3 ± 0.5	2.8 ± 0.2	0.25 ± 0.02	98.7 ± 0.5	10497[e]	7.0×10^{-5}
		Tin	1.85 ± 0.69	1.3 ± 0.4	0.6 ± 0.0	1.17 ± 0.07	98.7 ± 0.4	955 ± 388	$8.4 \pm 4.4 \times 10^{-4}$
SUITO	1.2 ± 0.0	Indium	0.41 ± 0.13	0.2 ± 0.1	0.6 ± 0.1	1.21 ± 0.18	99.8 ± 0.1	2673 ± 1104	$2.9 \pm 1.0 \times 10^{-4}$
		Tin	0.54 ± 0.04	0.4 ± 0.1	0.5 ± 0.1	1.47 ± 0.16	99.6 ± 0.1	4653 ± 1520	$1.6 \pm 0.7 \times 10^{-4}$
VD	1.1 ± 0.0	Indium	6.96 ± 2.00	5.2 ± 1.6	0.1 ± 0.1	6.15 ± 3.81	94.9 ± 1.6	239 ± 60	$3.1 \pm 0.0 \times 10^{-3}$
		Tin	15.64 ± 0.72	11.4 ± 1.9	0.5 ± 0.1	1.48 ± 0.25	88.6 ± 1.9	126 ± 81	$6.9 \pm 0.0 \times 10^{-3}$
RB	2.9 ± 0.0	Indium	7.23 ± 1.28	8.1 ± 1.9	2.3 ± 0.4	0.31 ± 0.05	91.9 ± 1.9	825[e]	8.4×10^{-4}[e]
		Tin	2.75 ± 0.59	1.9 ± 0.4	0.8 ± 0.4	0.93 ± 0.33	98.1 ± 0.4	535 ± 122	$1.3 \pm 0.3 \times 10^{-3}$

[a] f_r and f_s = the proportion of the total element dissolved in the initial rapid (f_r) or latter slower (f_s) phase; s_r and s_s = the dissolution rate for the initial rapid (s_r) or later slower (s_s) phase; $t_{1/2}$ = particle dissolution half-time.

[b] $In(OH)_3$ = indium hydroxide; In_2O_3 = indium oxide; SnO_2 = tin oxide; UITO = unsintered ITO; SITO = sintered ITO; SUITO = sintered/unsintered ITO; VD = ventilation dust; RB = reclaim byproduct.

[c] SSA = specific surface area as reported previously (Badding et al., 2014); <indicates that a precise value was not reported due to trade secret considerations.

[d] Cum = cumulative total elemental mass dissolved during seven-day study period.

[e] Fitted model did not converge for all replicate samples so parameter estimates were calculated using remaining samples.

Table 2

Dissolution of indium from industrially sampled powders (n = 3 samples per cell) in PSF (pH 4.5).

				Dissolution parameters (Mean ± Standard deviation)[a]					
				Initial rapid phase			Latter slower phase		
Material[b]	**SSA (m^2/g)**[c]	**Element**	**Cum (%)**[d]	f_r (%)	$t_{1/2}$ (d)	s_r (d^{-1})	f_s (%)	$t_{1/2}$ (d)	s_s (d^{-1})
In_2O_3	<5	Indium	1.87 ± 0.55	0.03 ± 0.05	0.41 ± 0.60	7.9 ± 6.4	100 ± 0.05	1880 ± 266	$3.7 \pm 0.5 \times 10^{-4}$
SITO	3.0 ± 0.1	Indium	4.85 ± 0.19	0.11 ± 0.10	0.20 ± 0.16	4.7 ± 2.5	99.9 ± 0.1	417 ± 18	$1.7 \pm 0.0 \times 10^{-3}$
VD	1.1 ± 0.0	Indium	15.43 ± 2.36	8.0 ± 1.5	0.10 ± 0.01	7.1 ± 0.9	92.0 ± 1.5	251 ± 85	$3.0 \pm 1.2 \times 10^{-3}$

[a] f_r and f_s = the proportion of the total element dissolved in the initial rapid (f_r) or latter slower (f_s) phase; s_r and s_s = the dissolution rate for the initial rapid (s_r) or latter slower (s_s) phase; $t_{1/2}$ = particle dissolution half-time.

[b] In_2O_3 = indium oxide; SITO = sintered ITO; VD = ventilation dust.

[c] SSA = specific surface area as reported previously (Badding et al., 2014); <indicates that a precise value was not reported due to trade secret considerations.

[d] Cum = cumulative total elemental mass dissolved during 28 day study period.